Studies on the Mechanism of the Instability of Polymers in Tensile Testing

JINAN CAO*

Department of Organic and Polymeric Materials, Tokyo Institute of Technology, Tokyo, Japan

SYNOPSIS

This study deals with the mechanism of the instability of tensile force occurring in tensile testing for polymer materials. It was found that through a proper transformation of inertia coordinates, a tensile test can be described in the same governing differential equations with the same boundary conditions as those employed in melt spinning. This fact suggests that the nature of the instability is simply due to draw resonance rather than any other cause. The effects of extension rate in tensile testing and the specimen dependence on the instability of tensile force were experimentally investigated by using specimens with various molecular orientations. The results are interpreted by applying the principles of draw resonance in melt spinning.

INTRODUCTION

There are two characteristic instability phenomena occurring in polymer processing and testing. One is the phenomenon called draw resonance in which cyclic variation of taken-up filament diameter or film thickness occurs in melt spinning or film-forming process despite maintaining constant process conditions. The other is the well-known tensile force oscillation phenomenon occurring in tensile testing, although all the test conditions are kept constant when necking deformation of a specimen occurs. Draw resonance appears to have been reported in the early 1960s.[1-5] The tensile force oscillation phenomenon, however, has a long history and was first discovered in the tensile test of metals.[6,7] It was in the 1950s that the tensile force oscillation phenomenon was also reported in polymer materials.[8,9] Especially in the case of polymers, this phenomenon is usually accompanied by optical and dimensional cyclical variations in tested specimens and has received considerable attention[10-12] by investigators in the fields of materials science and engineering. On the other hand, draw resonance has been mainly dealt with by researchers in the fields of rheology and polymer processing by means of mathematical analysis. Yet there has been no effort to establish the relationship between the two characteristic instabilities.

To elucidate the mechanism of molecular structure formation in melt spinning of polymers, the mathematical model of melt spinning has been extensively studied. The governing equations of melt spinning, describing the relationship between filament parameters such as the cross-sectional area, velocity, temperature, and viscosity, were established in the 1960s. They consist of simultaneous nonlinear partial differential equations and cannot be solved analytically except in a few special cases. Fortunately, the governing equations can be solved numerically by means of computer simulation. The numerical simulation of the governing equations in steady states was studied by Kase and Matsui[13,14] and has played an important role in interpreting the mechanism of molecular structure formation of polymers in melt spinning. Furthermore the numerical simulation was applied to transient states of melt spinning, and from the results of the simulation many essential features of draw resonance have been understood.[15-21] In fact, the governing equations have become an absolutely necessary tool in studying the mechanism of draw resonance in melt spinning.

* Present address: CSIRO Division of Coal & Energy Technology, P.O. Box 136, North Ryde, N.S.W. 2113 Australia.

Journal of Applied Polymer Science, Vol. 45, 2169–2179 (1992)
 CCC 0021-8995/92/122169-11$04.00

This powerful mathematical method, however, has never been introduced to solving the tensile force oscillation phenomenon in tensile testing. To explain this instability, Bunn and Alock[22] suggested a mechanism involving the tearing apart and rebuilding of crystalline regions of a specimen. Unfortunately, it is not essential for a filament to be crystalline to show the instability. In fact, amorphous filaments are much more unstable than crystalline filaments.

A common interpretation for the instability assumes the thermal effect on the mechanical behavior of a specimen.[23-26] According to this point of view, the energy introduced by the work of deformation during tensile testing will be converted into heat, which causes a local increase of temperature. It is the local increase of temperature that makes the tensile force decrease. Since necking deformation is propagated throughout the specimen, a low temperature of the new necking zone leads to an increase of tensile force, and this process can be iterated. This explanation is identical in principle to the "heat effect" of draw resonance in melt spinning.[3]

Another simple model for this instability without consideration of heat generation during necking deformation has been proposed by Pakula and Fischer.[27] The process of local rearrangement of molecular chain segments during necking deformation was believed to overcome an activation barrier. Based on thermodynamic analysis, Pakula and Fischer proposed that the instability is somewhat of a "spinodal transition" from an isotropic state into a highly oriented state.

Behary and Porcher[28] investigated the effects of molecular orientation and crystallization of polyethylene filaments on this instability. Their results showed that the extension rates of tensile tests and the molecular orientation degrees of specimens had the greatest effects on the occurrence of the unstable phenomenon.

In this present study, the tensile force oscillation phenomenon is first theoretically analyzed by establishing the governing equations of tensile testing during necking deformation. Inertia coordinates transformation points out that there is a common feature existing between the tensile force oscillation phenomenon and draw resonance in melt spinning. The decisive role of the mathematical analysis in elucidating the mechanism of the instability will be emphasized. The effects of extension rate and extension ratio of a tensile test and the molecular orientation degree of a specimen on the instability have been investigated, and the results interpreted by means of the principles of draw resonance in melt spinning. Although the discussion is restricted for polymer specimens, this analysis is believed to be also applicable for metals.

THEORETICAL

Governing Equations of Tensile Testing during Necking Deformation

In a manner similar to that used in melt spinning, the local velocity and stress as well as cross-sectional area of a specimen in tensile testing can be described in Eulerian coordinates. Figure 1 defines the parameters of the specimen in tensile testing. Obviously, the one-dimensional continuity equation can be written

$$\frac{\partial A(x,t)}{\partial t} + \frac{\partial [A(x,t)v(x,t)]}{\partial x} = 0 \qquad (1)$$

where $A(x, t)$ and $v(x, t)$ denote, respectively, the cross-sectional area and velocity of the specimen at time t and distance x, from the cross head of a tester. The density changes of the specimen during tensile testing have been disregarded because the changes are small.

In order to describe the plastic flow behavior of the necking zone of a specimen during necking deformation, the Trouton elongational viscosity can be introduced into tensile testing like in melt spinning.

$$\frac{\partial v(x,t)}{\partial x} = \frac{F(t)}{A(x,t)\beta(x,t)} \qquad (2)$$

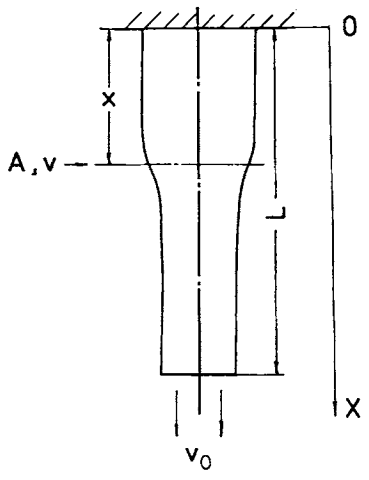

Figure 1 Parameters in tensile testing in stationary coordinates.

where $F(t)$ denotes the tensile force and is a constant along the specimen. When the instability of tensile force occurs, however, $F(t)$ oscillates with time t. The onset of the instability occurs mathematically because $F(t)$ is able to vary with time. The symbol β represents the Trouton elongational viscosity of the specimen during necking deformation when the specimen has already yielded. In general, β is not a constant; it depends in a complex way on the stain rate, temperature, and molecular orientation and crystallization of the specimen. In the nonnecking deformation zone of the specimen, β approaches infinity since it is an elastic deformation rather than a plastic flow.

Equations (3) and (4) are, respectively, the initial and boundary conditions of tensile testing.

$$v(x, t) = 0 \quad \text{when} \quad x = 0 \tag{3}$$

$$v[L(t), t] = V_0 \quad \text{where} \quad L(t) = L_0 + V_0 t \tag{4}$$

where V_0 and L_0 denote the extension rate and initial gauge length of tensile testing, respectively. $L(t)$ is the specimen length at time t.

The continuity equation (1) and the constitution equation (2) are the governing equations for tensile testing. Unsteady solutions of $F(t)$ will mathematically show the instability of tensile testing. Unfortunately, as in the case of melt spinning, they are given in a simultaneous nonlinear differential form and have not yet been solved analytically. Thus, comparing these equations with those used in melt spinning will be emphasized in analyzing the mechanism of the instability in tensile testing.

Equations (1) and (2) have the same forms as those employed in an isothermal melt spinning under constant spinning tension, but the initial and boundary conditions are different. It is well known that if initial and/or boundary conditions are different, there will be a completely different solution for partial differential equations. Therefore, it is necessary to further transform the relative inertia coordinates system.

Coordinates Transformation

When necking deformation occurs in tensile testing, the propagation velocity of the neck along a specimen can be calculated from the material balance equation.

As shown in Figure 2 (a),

$$A_0 L_0 \simeq A_0 y + A_1 x \tag{5}$$

$$L_0 + V_0 t = y + x \tag{6}$$

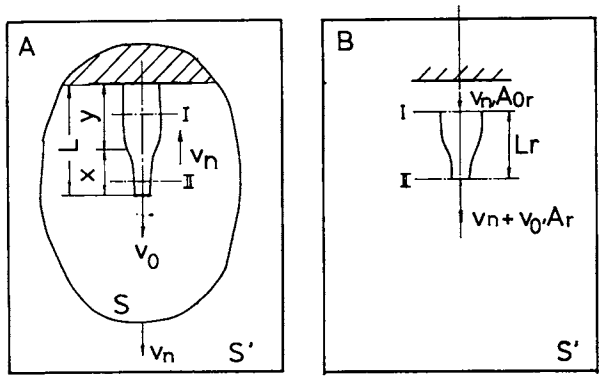

Figure 2 Coordinates transformation from the stationary coordinates S to a relative inertia coordinates S'.

The neck propagation velocity v_n is

$$v_n = -\frac{dy}{dt} = \frac{V_0}{n-1} \tag{7}$$

where n denotes the neck ratio, which is described as

$$n = \frac{A_0}{A_1} \tag{8}$$

where A_0 and A_1 are the cross-sectional areas of the specimen sections above and below the neck, respectively. Therefore, v_n is a function of the neck ratio, which is in turn determined by the material properties of the specimen.

If one observes the specimen in a coordinates system S' which is moving at velocity $\mathbf{v}_n$ relative to the stationary coordinates S, the neck propagation becomes stationary relative to the coordinates S'. Consequently, the dynamic behavior of tensile testing can be described in the same way as that in melt spinning. This is to say, plan I in Figure 2(a) can be thought of as a spinneret from which polymer fluid is extruded at the velocity v_n with the cross-sectional area A_{0r}. Plan II, can be considered as a take-up point at which polymer fluid is taken up at the velocity $v_n + v_0$ with the cross-sectional area A_r [Fig. 2 (b)]. Therefore, it is obvious that tensile testing can be thought of as one kind of melt spinning with an appropriate coordinates transformation. Thus it is clear that it is draw resonance that the mechanism of the instability lies in.

In the relative inertia coordinates, S', the draw ratio is written as

$$\psi_w = n = \frac{V_n + V_0}{V_n} = \frac{A_{0r}}{A_r} \tag{9}$$

Supposing the necking phenomenon shown in Figure 3(a) occurs as well, the neck propagation velocity is then written as

$$V_n = \frac{dx}{dt} = \frac{nV_0}{n-1} \tag{10}$$

In the relative inertia coordinates, which are moving at $\mathbf{v}_n$ relative to the stationary coordinates, the following draw ratio can be obtained:

$$\psi_w = n = \frac{V_n}{V_n - V_0} = \frac{A_{0r}}{A_r} \tag{11}$$

As a result, in both the cases of Figures 2 and 3, the governing equations of tensile testing may have identical mathematical forms to melt spinning with a proper coordinates transformation. Note that the draw ratio in the relative coordinates S' has a different definition from the extension ratio in tensile testing, viz., the extension rate divided by the initial specimen length. In the following, only the case of Figure 2 will be discussed.

The governing equations in the relative inertia coordinates S' become

$$\frac{\partial A_r(x_r, t)}{\partial t} + \frac{\partial [A_r(x_r, t) v_r(x_r, t)]}{\partial x_r} = 0 \tag{12}$$

$$\frac{\partial v_r(x_r, t)}{\partial x_r} = \frac{F(t)}{A_r(x_r, t)\beta(x_r, t)} \tag{13}$$

The initial and boundary conditions are then written

$$v_r(0, t) = V_n \quad \text{and} \quad A_r(0, t) = A_{0r} \quad \text{when} \quad x_r = 0 \tag{14}$$

$$v_r(L_r, t) = V_n + V_0 \quad \text{when} \quad x_r = L_r \tag{15}$$

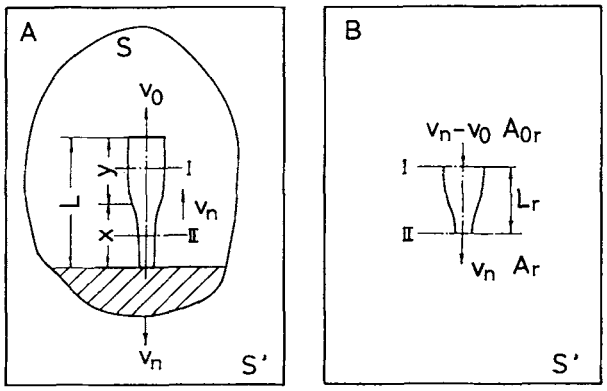

Figure 3 Coordinates transformation from the stationary coordinates S to a relative inertia coordinates S' (another case).

Table I Main Melt Spinning Conditions

Polymer	Spinning Temp. (°C)	Flow Rate (g/min)	Take-up Velocity (m/min)
PET	293	4.0	1000
			3000
			5000

where the subscript r denotes the relative inertia coordinates.

Equations (12) and (13) are simultaneous nonlinear partial differential equations like those used in melt spinning, and analytical solutions cannot be achieved readily. However, based on the principles of draw resonance, one can interpret the instability without recourse to solving these equations. The consistencies of the governing equations as well as the initial and boundary conditions for tensile testing with those used in melt spinning suggest that the instability has the same mechanism as draw resonance. Therefore, it is anticipated that the instability may be interpreted by employing the principles of draw resonance in melt spinning.

In a previous paper by the author,[29] the cross-sectional area dependence of the local draw ratio, $\frac{\partial}{\partial A}(\partial v/\partial x)$, was demonstrated to be the necessary condition of draw resonance in melt spinning. According to whether the value of $\frac{\partial}{\partial A}(\partial v/\partial x)$ is positive or negative, the filament drawing can be defined as a uniformizing draw mode or a nonuniformizing draw mode. In the case of tensile testing, the nonuniformizing draw mode corresponds to strain softening, and the uniformizing draw mode corresponds to strain hardening. When necking deformation occurs in tensile testing, the decrease of the cross-sectional area caused by yielding makes the true stress increase. Consequently, the strain softening effect stretches the section with a smaller cross-sectional area to a larger extent. On the other hand, the Trouton elongation viscosity increases abruptly with the plastic flow deformation of a necking specimen because of the increase of molecular orientation and

Table II Birefringence of Specimens

Specimen (m/min)	$\Delta n \times 10^3$
1000	5.0
3000	29.0
5000	90.0

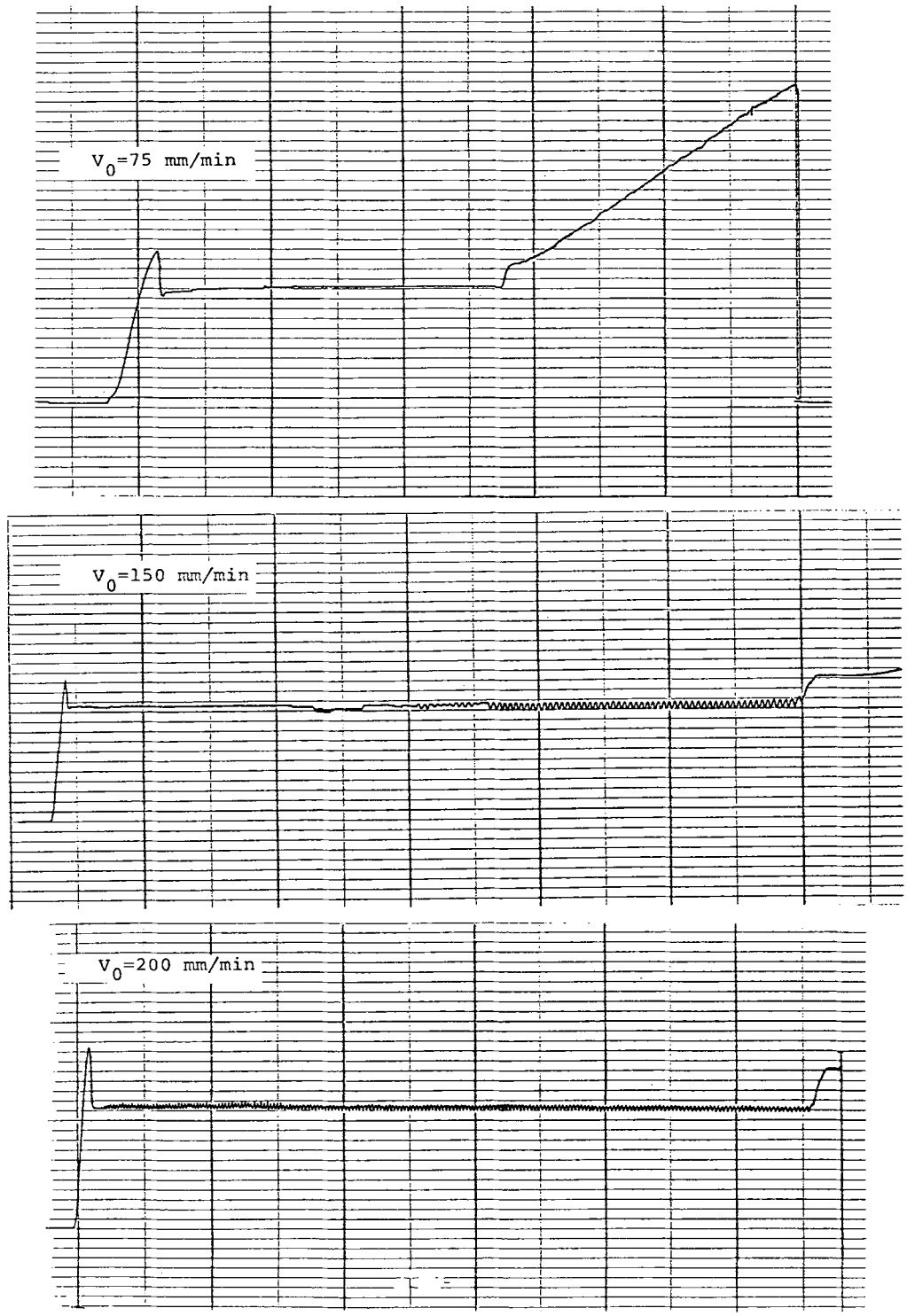

Figure 4 Load-extension curves for the PET fiber specimens with low molecular orientation at various extension rates.

orientation-induced crystallization of the specimen. As compared with the increase of the true stress, when the increase of the Trouton elongational viscosity becomes dominant, further stretch for the smaller sections halts. The strain softening effect shows why necking deformation occurs, and the strain hardening effect, on the other hand, explains why the specimen does not break. Whether the in-

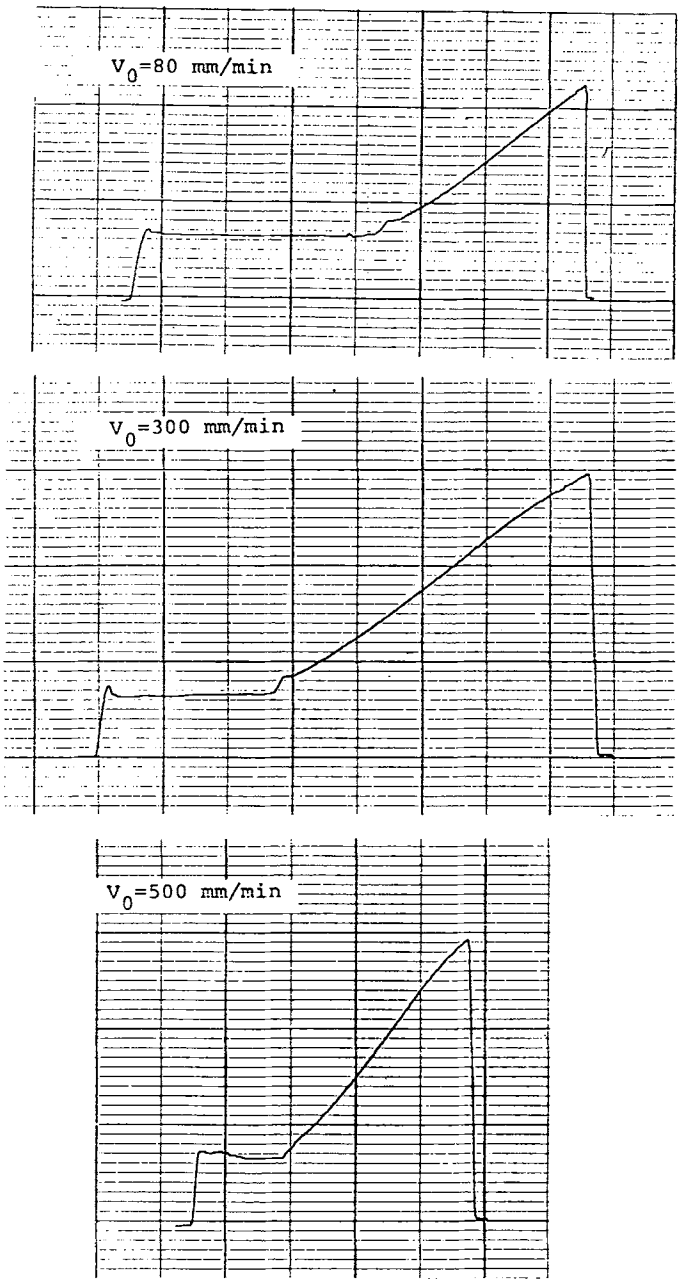

Figure 5 Load-extension curves for the PET fiber specimens with medium molecular orientation at various extension rates.

EXPERIMENTAL

Specimens

Filaments were prepared by melt spinning polyeth- and 5000 m/min were tested, and they were referred to as the specimens with low, medium and high molecular orientations, respectively. Melt spinning was carried out at the laboratory of the Tokyo Institute of Technology. The main melt spinning conditions are listed in Table I. For the detailed spinning conditions one may refer to the cited literature.[30,31]

Optical Analysis

The refractive indices parallel and perpendicular to the filament axis ($n_{\parallel}$ and $n_{\perp}$) were measured by using

an interference microscope (Carl Zeiss, Jena) with a polarization filter. Birefringence Δn was then calculated as $\Delta n = n_{\parallel} - n_{\perp}$. In addition, a polarization microscope equipped with a Na D-line light source was employed to investigate the development of molecular orientation of the necking zone for unloaded specimens. Furthermore, a neck surface of an unloaded specimen was investigated by using a JSM T-200 scanning electron microscope.

Tensile Testing

Tensile testing was performed in a Tensilon tensile tester at room temperature in air. The gauge lengths of 20, 40, and 60 mm and the extension rates from 20 to 500 mm/min were employed. Tensile force during tensile testing was recorded on electromagnetic recording charts.

RESULTS AND DISCUSSION

Table II shows birefringence for the three kinds of specimens used in this study. By simply increasing the spinning velocity, the as-spun fibers showed low oriented, medium oriented, and highly oriented structures in sequence. In Figure 4 the tensile forces for the low oriented specimen (1000 m/min, specimen length 40 mm) during tensile testing are displayed. When the extension rate was low, no tensile force oscillation phenomenon was observed. With the extension rate increasing, however, the tensile force started to oscillate from the middle of the load-extension curve, then continued with a standing period and amplitude. At the 200-mm/min extension rate, the tensile force appeared to oscillate as soon as necking deformation appeared. These phenomena completely correspond to the concept of the limit cycle of draw resonance in melt spinning,[20,21,31] which maintains that if the draw ratio in melt spinning is higher than a critical draw ratio of draw resonance, there is a standing oscillation having certain amplitude and period independent of the initial conditions.

Figures 5 and 6 show the load-extension curves for the specimens of 3000 and 5000 m/min during testing (specimen length 40 mm). No tensile force oscillation was observed in the whole range of the extension rates employed.

The influence of gauge length for the 1000 m/min specimen is shown in Figure 7. The abscissa is the extension rate and the ordinate the extension ratio of testing. These experimental results indicate that it is the extension rate rather than the extension ratio that the instability depends on.

In order to study the structure changes of the specimens during tensile testing, a specimen of low orientation (gauge length 40 mm, extension rate 200 mm/min) was unloaded from the tester when necking deformation was propagating. A polarization micrograph for this specimen is shown in Figure 8. It is seen that with the development of deformation of the neck birefringence of the specimen develops. Since the same order of interference fringe has the same quantity of the difference of optical distance, the interference fringes vertical to the fiber axis in the necking zone seem to demonstrate that molec-

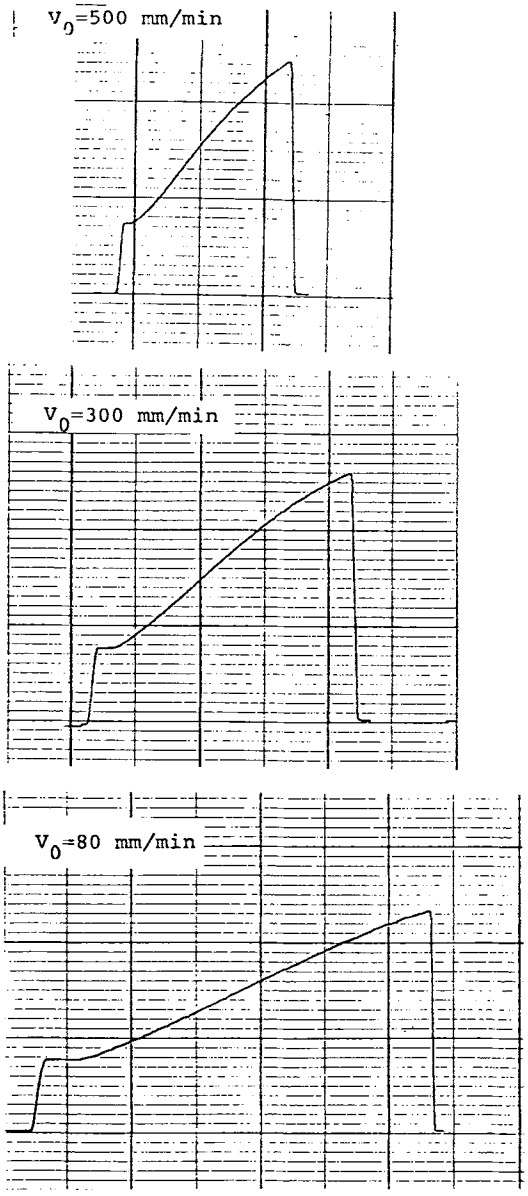

Figure 6 Load-extension curves for the PET fiber specimens with high molecular orientation at various extension rates.

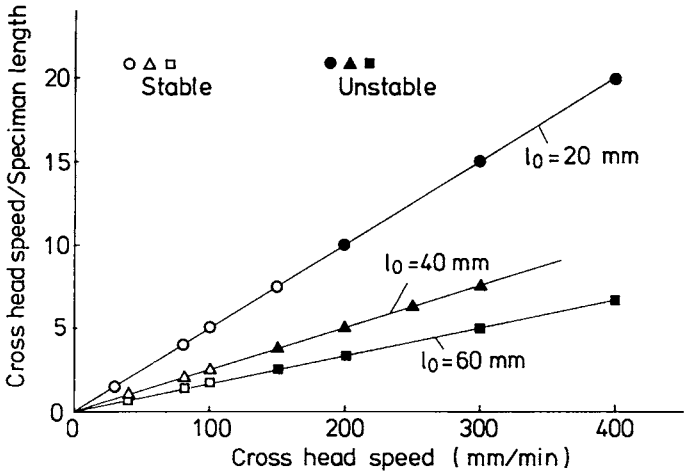

Figure 7 The tensile force oscillation phenomenon depends on the extension rates rather then the extension ratios.

ular orientation of the specimen began from the skin layer first, then spread to the core layer. The central interference fringe shows clearly periodical variation along the fiber axis, and the product of the length of the period and the number of the tensile force oscillation peaks in the load-extension curve was equal to the specimen length. Thus, it is clear that the periodical variation of molecular orientation of the specimen was caused by the instability. On the other hand, no such cyclical change of the interference fringes was found for a stable tensile test.

The above experimental results can be summarized in two points. One is the specimen dependence and the other is the extension rate dependence of the instability. The results can be explained using the analytical method proposed in the previous paper.[29] In the relative inertia coordinates S', as shown in Figure 2, when necking deformation occurs, the upper parts of a specimen are at rest and the lower parts are taken-up at velocity of $v_n + v_0$. Only the zone between plan I and II is involved in the coordinates S'. The instability has nothing to do with gauge length. The mathematical analysis method used in the analysis of draw resonance in melt spinning is, in principle, applicable to the instability analysis of tensile testing as well.

Figure 9 illustrates a diameter profile of a specimen during necking deformation, as well as the profiles of the velocity and velocity gradient in the relative inertia coordinates S'. The velocity gradient increases with the distance from the neck starting point, reaches the maximum, and then decreases. On the left side of the maximum velocity gradient point, there is $\partial^2 v_r/\partial x_r^2 > 0$; it is the strain softening region. On the right side, $\partial^2 v_r/\partial x_r^2 < 0$; it corresponds to the strain hardening region. The strain softening region is the promotive factor, and the strain hardening region becomes the suppressive factor for the instability. Whether the instability phenomenon occurs will depend on the competition of strain softening and strain hardening.

This mathematical analysis plays a decisive role in studying the mechanism of the instability of tensile testing, rather than establishing a quantitative method. First of all, the one-dimensional governing equations are very precise for melt spinning but not accurate enough for tensile testing because necking deformation occurs in a very short range along a specimen, suggesting that three-dimensional equations should be used. Figure 8 has already illustrated that birefringence of the necking zone develops three dimensionally, implying a difference of the Trouton viscosities from the skin layer to the center layer. Figure 10 is a scanning electron micrograph of the necking zone for an unloaded specimen. As can be seen, there were many wrinkles on the surface of the specimen, providing further evidence. Second, it is not easy to obtain accurately $\partial/\partial A_r(\partial v_r)\partial x_r)$ from experimental data. Consequently, to calculate the stable parameter as in melt spinning is difficult in practice. The mechanism of the instability is thought to be more important than a quantitative analysis.

The mathematical explanation can be related to the molecular interpretation of the instability. As compared with the specimen of 1000 m/min, molecules of the specimens of 3000 and 5000 m/min have already oriented to certain extents. One reason,

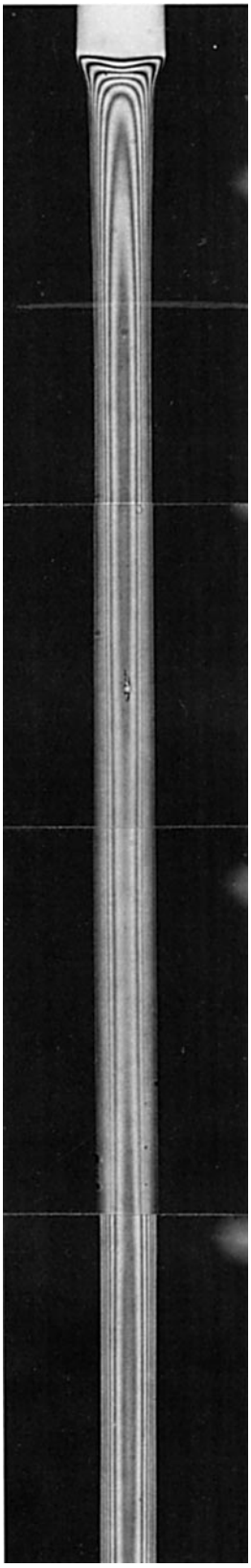

Figure 8 A polarization micrograph for the necking zone of an unloaded specimen (unstable).

therefore, could be that the Trouton elongational viscosity increases only slightly with stretching for low orientation specimens and increases abruptly for high orientation specimens. This reason is in good agreement with the fact that a highly oriented specimen will have much higher yield stress than a low oriented specimen. Therefore during necking deformation, the strain hardening effect will be detected earlier for the specimens whose molecules have already oriented to some extent but later for the specimen whose molecules have not oriented yet. It is then anticipated that the strain hardening effect for the specimen having a larger neck ratio is delayed. From the relationship between the nature extension ratio and the neck ratio, one will easily understand that the specimens of 3000 and 5000 m/min have a weaker strain softening effect than the specimens of 1000 m/min. This is why the medium and highly oriented specimens were much more stable than the low oriented specimen.

The extension rate dependence of the instability could lie in the positive correlation between the strain softening effect and extension rate. Figure 11 is a plot of the neck ratios against the extension rates for the specimens of 1000 m/min. It is seen from the plot that the higher the extension rate, the greater is the neck ratio. This fact suggests that the strain softening effect was larger in a tensile test with higher extension rate. Smith and Ender et al.[32–34] demonstrated that there is a delay time for molecular rearrangement of a specimen under a constant load tensile test. As compared with the strain rate of the specimen, the retardatory time of molecular orientation of the specimen is longer for higher extension rates. Consequently, the strain hardening effect was retarded, and the instability occurred in higher extension rate tests.

It should be pointed out that the mechanism of the instability is applicable not only to polymer materials but also to metals. However, metals are crystalline, and their strain hardening effects are realized by dislocations.

CONCLUSION

The governing equations for tensile testing during necking deformation consist of the continuity equation (1) and the constitution equation (2). By a relative inertia coordinates transformation, it was shown that these partial differential equations have the same mathematical forms with the same initial and boundary conditions as those used in isothermal melt spinning under uniform tension. This fact sug-

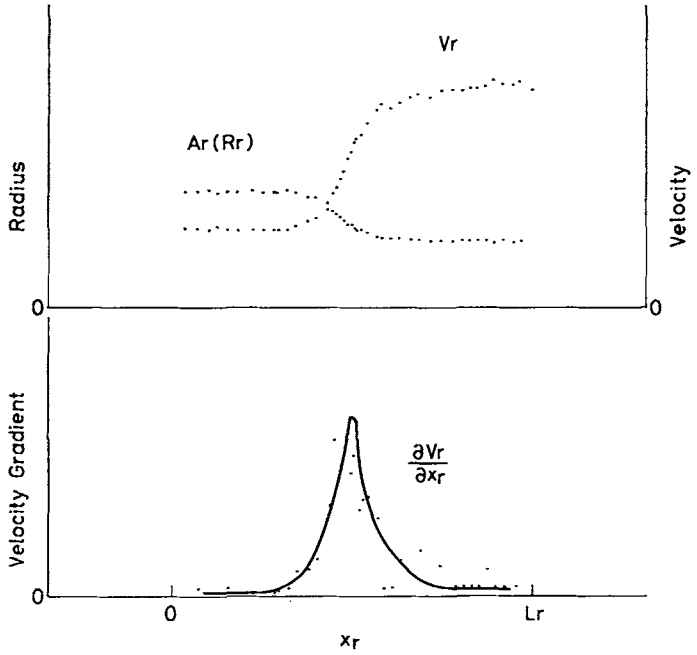

Figure 9 Radius, velocity, and velocity gradient profiles of a necking zone in the relative inertia coordinates S'. The radius profile was measured by using an unloaded specimen.

gests the instability in tensile testing is simply due to draw resonance rather than any other cause. However, the abrupt change of the cross-sectional area and the stress concentration of a specimen in the necking zone orient molecules in the skin layer of the specimen earlier than the central layer. One-dimensional equations are not sufficient to quantitatively describe the dynamic behavior of a specimen in tensile testing. The instability is dominated by the competition of the effects of strain softening and

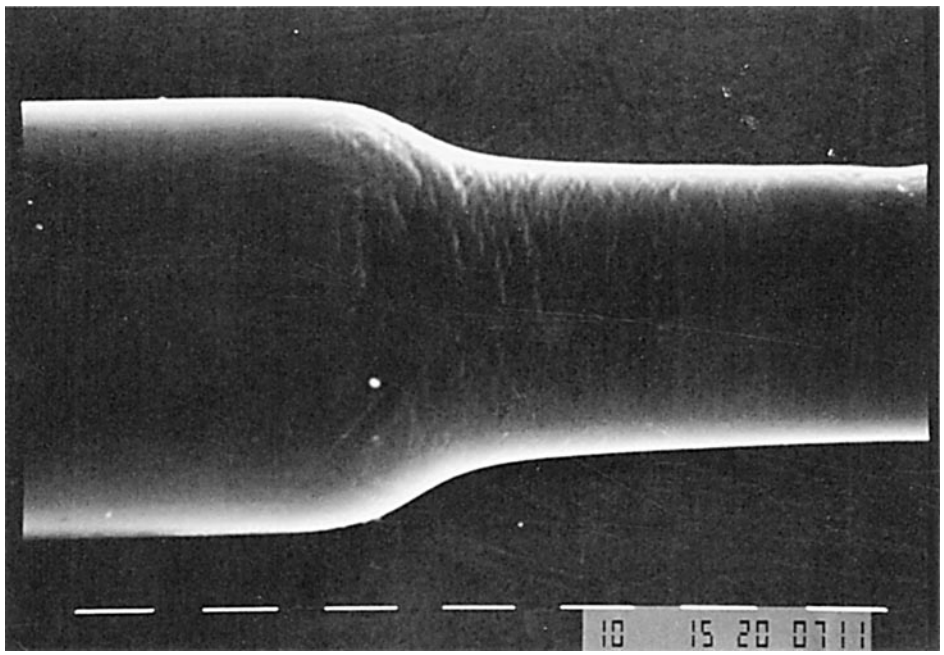

Figure 10 A SEM photograph for the surface of the necking zone of an unloaded specimen.

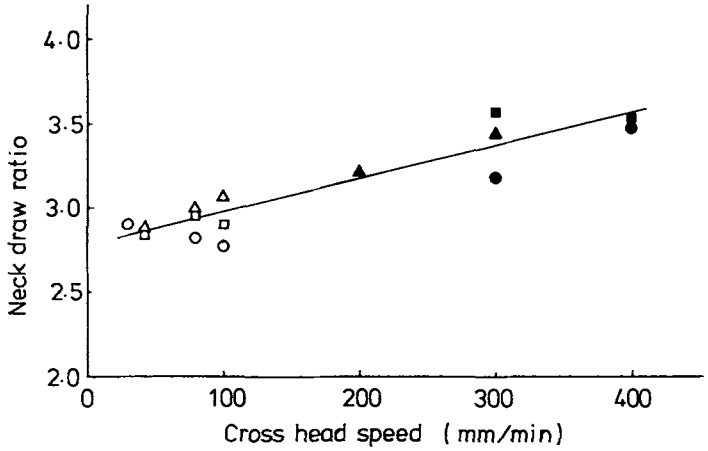

Figure 11 Relationship between the neck ratio of a specimen and the extension rate in tensile testing.

strain hardening. Because the strain softening effect for a partially and highly oriented specimen was weak, no tensile force oscillation was observed. However, as compared with the strain rate in the case of higher extension rate, the delay time of molecular orientation became longer, the strain softening effect was strong and the instability occurred.

REFERENCES

1. R. E. Christensen, *SPEJ,* **18,** 571 (1962).
2. J. C. Miller, *SPE Trans.,* **3,** 134 (1963).
3. H. I. Freeman and M. J. Coplan, *J. Appl. Polym. Sci.,* **8,** 2389 (1964).
4. C. J. S. Petrie and M. M. Denn, *AIChE J.,* **22,** 209 (1976).
5. C. D. Han and Y. W. Kim, *J. Appl. Polym. Sci.,* **20,** 1555 (1976).
6. B. Chalmer, *Physical Metallurgy,* Wiley, New York, 1962, p. 401.
7. G. E. Dieter, Jr., *Mechanical Metallurgy,* McGraw-Hill, New York, p. 135.
8. I. Marshall and A. B. Thompson, *Proc. Roy. Soc.,* **A-221,** 541 (1954).
9. D. C. Hookway, *J. Text. Inst. Proc.,* **49,** 7 (1958).
10. D. C. Hookway, *J. Text. Inst. Proc.,* **49,** 292 (1958).
11. R. Roseen, *J. Mater. Sci.,* **9,** 929 (1974).
12. M. J. Napolitano and A. Moet, *J. Appl. Polym. Sci.,* **34,** 1285 (1985).
13. S. Kase and T. Matsuo, *J. Polym. Sci.,* **A3,** 2541 (1965).
14. S. Kase and T. Matsuo, *J. Polym. Sci.,* **11,** 251 (1967).
15. S. Kase, *J. Appl. Polym. Sci.,* **18,** 3279 (1974).
16. J. R. A. Pearson and Y. T. Shah, *Ind. Eng. Chem. Fundam.,* **8,** 605 (1969).
17. Y. T. Shah and J. R. A. Pearson, *Ind. Eng. Chem. Fundam.,* **11,** 145 (1972).
18. Y. T. Shah and J. R. A. Pearson, *Ind. Eng. Chem. Fundam.,* **11,** 150 (1972).
19. Y. T. Shah and J. R. A. Pearson, *J. Polym. Eng. Sci.,* **12,** 219 (1972).
20. H. Ishihara and S. Kase, *J. Appl. Polym. Sci.,* **19,** 557 (1975).
21. H. Ishihara and S. Kase, *J. Appl. Polym. Sci.,* **20,** 169 (1976).
22. C. W. Buun and T. C. Alock, *Trans. Farad. Soc.,* **4,** 317 (1945).
23. P. H. Muller and A. Engelter, *Klloid Z.,* **150,** 156 (1957).
24. G. P. Andrianova, A. S. Kechekyan, and V. A. Kargin, *J. Polym. Sci., A2,* **9,** 1919 (1971).
25. G. I. Barenblat, in H. H. Kansch, Ed., *Deformations and Fracture of High Polymers,* Plenum, New York, 1973.
26. G. P. Andrianova, B. A. Arutyunov, and Yu. V. Popov, *J. Polym. Sci. Polym. Phys. Ed.,* **16,** 1139 (1978).
27. J. Pakula and E. W. Fischer, *J. Polym. Sci. Polym. Phys. Ed.,* **19,** 1705 (1981).
28. H. M. Behery and B. K. Porcher, *J. Engin. Ind.,* **104,** 175 (1982).
29. J. Cao, *J. Appl. Polym. Sci.,* **42,** 143 (1991).
30. J. Shimizu, K. Toriumi, and K. Tamai, *Sen-i Gakkashi,* **33,** T-208 (1977).
31. J. Shimizu, N. Okui, and T. Kikutani, in A. Ziabicki and H. Kawai, Eds., *High-speed Fiber Spinning,* Wiley, New York, 1985.
32. F. S. Smith, *J. Phys., D, Appl. Phys.,* **8,** 759 (1975).
33. D. H. Ender and R. D. Andrews, *J. Appl. Phys.,* **36,** 3057 (1965).
34. D. H. Ender, *J. Appl. Phys.,* **39,** 4877 (1968).

Received May 3, 1991
Accepted August 12, 1991